

On the decadal scale correlation between African dust and Sahel rainfall: The role of Saharan heat low–forced winds

Weijie Wang, Amato T. Evan, Cyrille Flamant, Christophe Lavaysse

► **To cite this version:**

Weijie Wang, Amato T. Evan, Cyrille Flamant, Christophe Lavaysse. On the decadal scale correlation between African dust and Sahel rainfall: The role of Saharan heat low–forced winds. *Science Advances*, American Association for the Advancement of Science (AAAS), 2015, 1 (9), pp.e1500646. 10.1126/sciadv.1500646 . insu-01214269

HAL Id: insu-01214269

<https://hal-insu.archives-ouvertes.fr/insu-01214269>

Submitted on 11 Oct 2015

HAL is a multi-disciplinary open access archive for the deposit and dissemination of scientific research documents, whether they are published or not. The documents may come from teaching and research institutions in France or abroad, or from public or private research centers.

L'archive ouverte pluridisciplinaire **HAL**, est destinée au dépôt et à la diffusion de documents scientifiques de niveau recherche, publiés ou non, émanant des établissements d'enseignement et de recherche français ou étrangers, des laboratoires publics ou privés.

On the decadal scale correlation between African dust and Sahel rainfall: The role of Saharan heat low–forced winds

Weijie Wang,¹ Amato T. Evan,^{1*} Cyrille Flamant,² Christophe Lavaysse³

A large body of work has shown that year-to-year variations in North African dust emission are inversely proportional to previous-year monsoon rainfall in the Sahel, implying that African dust emission is highly sensitive to vegetation changes in this narrow transitional zone. However, such a theory is not supported by field observations or modeling studies, as both suggest that interannual variability in dust is due to changes in wind speeds over the major emitting regions, which lie to the north of the Sahelian vegetated zone. We reconcile this contradiction showing that interannual variability in Sahelian rainfall and surface wind speeds over the Sahara are the result of changes in lower tropospheric air temperatures over the Saharan heat low (SHL). As the SHL warms, an anomalous tropospheric circulation develops that reduces wind speeds over the Sahara and displaces the monsoonal rainfall northward, thus simultaneously increasing Sahelian rainfall and reducing dust emission from the major dust “hotspots” in the Sahara. Our results shed light on why climate models are, to date, unable to reproduce observed historical variability in dust emission and transport from this region.

INTRODUCTION

By mass, aeolian dust is the most pervasive aerosol in the atmosphere (1). The presence of suspended dust affects the local energy balance through direct (2) and indirect effects (3), modifies the hydrological cycle via radiative forcing (4) and modification of cloud microphysical properties (5), and is a vehicle for the long-range transport of nutrients to global oceans (6) and terrestrial land surfaces (7). However, despite the importance of dust to the Earth system, coupled climate models are not able to reproduce historical variability in dust emission and transport (8), and thus, there is little confidence in projections of how atmospheric dust concentrations will change in the future. Hence, there is a need to understand the controls on historical changes in dust using observational data.

North Africa is the world’s largest dust source, accounting for more than 55% of global dust emissions (9, 10), and nearly 60% of the dust transported off the continent is deposited in the Atlantic Ocean (1). Long-term in situ observations at Barbados (11) and coral reef proxy and satellite data (12, 13) have shown that dust emission from North Africa peaked during the mid-1980s and has followed a downward trend through at least the late 2000s. Studies have found that dust cover over the Atlantic is anticorrelated with previous-year Sahelian precipitation (11), and a causal relationship between the decline in dust emission and the increase in Sahelian rainfall is plausible because increasing soil moisture would strengthen soil cohesion forces (14), and more dense vegetation cover would increase surface roughness (15), both acting to limit erosion and the mobilization of particles from the surface into the atmosphere. However, there are several aspects of such a theory that are not consistent. For example, satellite imagery suggests that most dust-emitting regions lie to the north of the vegetated region of the Sahel (10, 16), and in situ observations have shown that a more northward propagation of the monsoon, which

results in greater Sahelian rainfall, should increase the occurrence of dust emission from sources in the Sahel via haboobs (17). Additionally, a recent study demonstrated that the downward trend in dust that started in the mid-1980s could be reproduced in an aerosol emission and transport model when forced only by historical wind fields from reanalysis and when holding the Sahelian vegetation density constant (18).

Therefore, on the one hand, it would appear as though changes in surface winds over the hyperarid Sahara Desert should be sufficient to describe year-to-year changes in summertime dust emission, yet on the other hand, there is clear evidence showing that dust transported across the Atlantic is inversely proportional to rainfall, as well as vegetation density, in the Sahel. Here, we reconcile this contradiction by showing that both Saharan surface wind fields over the major regional dust-emitting regions and the northward propagation of the monsoon flow, and thus Sahel rainfall, are forced by the thermodynamic state of a meteorological feature termed the Saharan heat low (SHL).

RESULTS

Dust and precipitation

The Sahelian region of North Africa is an arid to semiarid region lying between the Sahara and the more tropical regions near the Guinea coast that is characterized by average summertime precipitation rates from 2 to 6 mm day⁻¹. Numerous studies have suggested that Atlantic dust cover is sensitive to rainfall in the Sahel, given the negative correlations between dust and monsoon season precipitation (11, 17). Indeed, the time series of summertime, June to August, the season when dust production peaks (19), with tropical North Atlantic dust aerosol optical depth (τ_d) estimated from satellites (12), shows that τ_d has been decreasing since the mid-1980s, whereas Sahelian rainfall, from the Global Precipitation Climatology Project (20), has been increasing over the same time period (Fig. 1). The time series of monsoon season Sahelian rainfall and satellite-retrieved τ_d , over the period 1982–2010, are statistically significantly correlated at an r value

¹Scripps Institution of Oceanography, University of California, San Diego, La Jolla, CA 92093, USA. ²Sorbonne Universités, UPMC (Université Pierre et Marie Curie) Université Paris 6, CNRS & UVSQ, UMR 8190 LATMOS, 75252 Paris, France. ³European Commission, Joint Research Centre, Ispra, Varese 21027, Italy.

*Corresponding author. E-mail: aeavan@ucsd.edu

of -0.53 ($P = 0.014$). Using dust concentration measurements from Barbados (11) and the same rainfall data, but over the period 1965–2009, the correlation between dust and precipitation is -0.52 .

The basis for the theory that Sahelian rainfall affects dust emission is that although the correlation between concurrent-year rainfall and dust is statistically significant and negative, the magnitude of the correlation between previous-year rainfall and dust is larger in magnitude (11) (-0.68 using satellite data and -0.66 using the

Barbados data). However, on the basis of the results from a Fisher’s z test to determine the significance of the difference in correlation coefficients, we cannot rule out the null hypothesis that the lagged correlations are statistically indistinguishable from the nonlagged correlations. That is, the fact that the correlation magnitude peaks when Sahelian rainfall leads dust by 1 year may simply be a statistical artifact.

The Saharan heat low

We next examine the concurrent roles of the SHL in dust emission and rainfall in the summer. The SHL is a region of a local surface and lower tropospheric temperature maximum and surface pressure minimum that is present in the western Sahara Desert during the summer (June to August) months, and is characterized by a broad low-level cyclonic circulation and mid-level anticyclonic circulation, about the SHL center (21) (Fig. 2A). The magnitude and extent of these two circulation features can be described by the atmospheric thickness between the 700- and 925-hPa levels, averaged spatially over the SHL center (Z_{hl}), using geopotential height from ERA-Interim reanalysis (22). Larger values of Z_{hl} indicate a strengthening of the characteristic SHL circulation features (21). The SHL center is detected in a manner identical to the Lagrangian SHL tracking method described in (21). The temperature and thickness of the SHL change on time scales ranging from synoptic (23) to interannual (24), and over the last three decades, Z_{hl} has increased (Fig. 1), a trend that is corroborated by in situ observations (24).

As the SHL warms and Z_{hl} increases, there is an intensification of the low-level cyclonic circulation that has its center of action about the SHL (23), and this strengthened low-level circulation increases

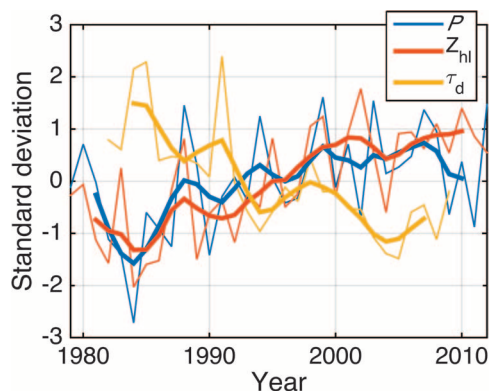


Fig. 1. Seasonal (June to August) time series of Z_{hl} (blue), precipitation (P , green), and τ_d (red). The monthly mean precipitation series is averaged over 5°W to 20°E , 10° to 20°N , and τ_d is averaged over 10° to 65°W and 0° to 30°N . The thin lines are the seasonal means, and the thick lines are the five-season smoothed time series (via a 1-4-7-4-1 filter).

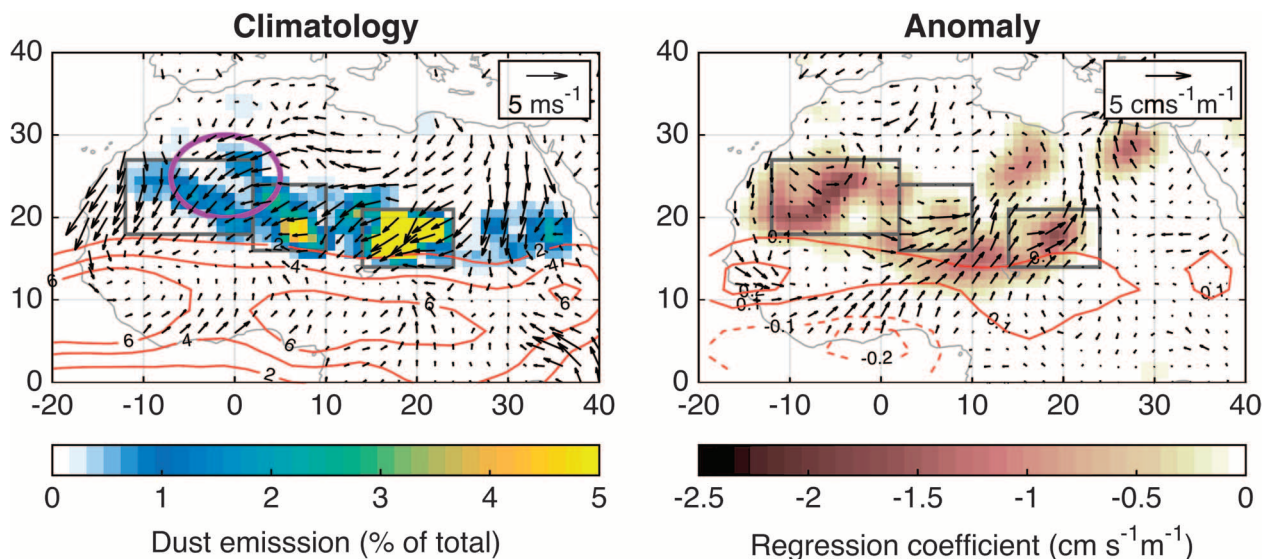


Fig. 2. Climatology and regressed precipitation and winds. (A) Shown is a map of long-term mean dust emission (shading), seasonal mean precipitation (magenta contour lines, mm day^{-1}), and seasonal mean 925-hPa climatological wind vectors (June to August). Dust emission rates are in nondimensional units of % of total annual mean of North Africa dust emission rates. The red circle indicates the location of the mean seasonal (June to August) position of the SHL. The brown boxes are the major dust hotspots of the Bodélé depression (14° to 24°E , 14° to 21°N), the depression in the lee of the Air and Adrar Mountains (2° to 10°E , 16° to 24°N), and the Mauritania and Western Sahara source region (12° to 2°W , 18° to 27°N , dashed lines). (B) Map of the coefficients of the regression of 925-hPa meridional and zonal winds (vectors and shading) and precipitation onto Z_{hl} , for June to August and 1979 through 2012. Vectors are all unit length to indicate anomalous wind direction, and the shaded regions are the wind speed coefficients, where only coefficients statistically significant at the 90% level are shown.

Sahelian rainfall during the monsoon season via a northward displacement of the monsoon flow (24). Covariability of Z_{hl} and precipitation is evidenced by a statistically significant correlation of their seasonal time series ($r = 0.54$, $P = 0.01$) (Fig. 1). This covariability is also seen in Fig. 2B, which shows coefficients of the regression of monthly precipitation anomalies onto monthly mean Z_{hl} anomalies, for the summer months (June to August) and from 1979 through 2012. Here, given an anomalously warm SHL, there is an increase in Sahelian precipitation and a reduction in rainfall along the Gulf of Guinea (Fig. 2B), indicating an anomalously northward position of the monsoon rain band, which is consistent with other studies (24). The dependency of the Sahelian rainfall on the intensity of the SHL is also evident in the regression of 925-hPa winds onto Z_{hl} , also for the months of the monsoon season, which show an anomalous low-level southwesterly flow between the Gulf of Guinea and the Sahel (Fig. 2B) that intensifies the climatological southerly monsoon flow (Fig. 2A) and thus increases the northward transport of moisture to the Sahel (24).

Simultaneous with the increase in Sahel rainfall that is associated with an anomalously warm SHL, there is also a reduction in wind speeds over the three most important dust-emitting regions of the Sahara: the Bodélé depression, a depression in the lee of the Air and Adrar Mountains, and western Mauritania and the Western Sahara (10, 16, 24, 25) (Fig. 2A). We note that although the dust emis-

sion map from (25) does not show high (relative) emission rates over Mauritania and the Western Sahara, another independent estimate of North African dust emission (10) suggests that this region has the highest emission rates for the entire region.

For all three major dust source regions, the climatological low-level winds are northerly to northeasterly (Fig. 2A), but the anomalous wind fields associated with an increase in Z_{hl} are southwesterly (Fig. 2B), a result of the anomalous cyclonic rotation about the SHL center of action. Consequently, as Z_{hl} increases and the SHL circulation strengthens, there is a net reduction in the scalar 925-mbar wind speeds over these important source regions, as evidenced by the statistically significant coefficients of the regression of wind speed onto Z_{hl} (shading, Fig. 2B). Thus, the regressions of monsoon rainfall and winds onto Z_{hl} (Fig. 2B) demonstrate that changes in the low-level circulation associated with the SHL can simultaneously increase Sahelian rainfall and reduce North African dust emission, via the well-established relationship between surface wind speeds and emission [for example, (14)].

Surface wind speeds during strong and weak SHL phases

To more clearly link the dynamics of the SHL to dust emission over the three major source regions (Fig. 3A), we created histograms of reanalysis (22) of six hourly 10-m wind speed for the 300 largest and 300 smallest daily values of Z_{hl} (Fig. 3, A to C). The surface wind speed

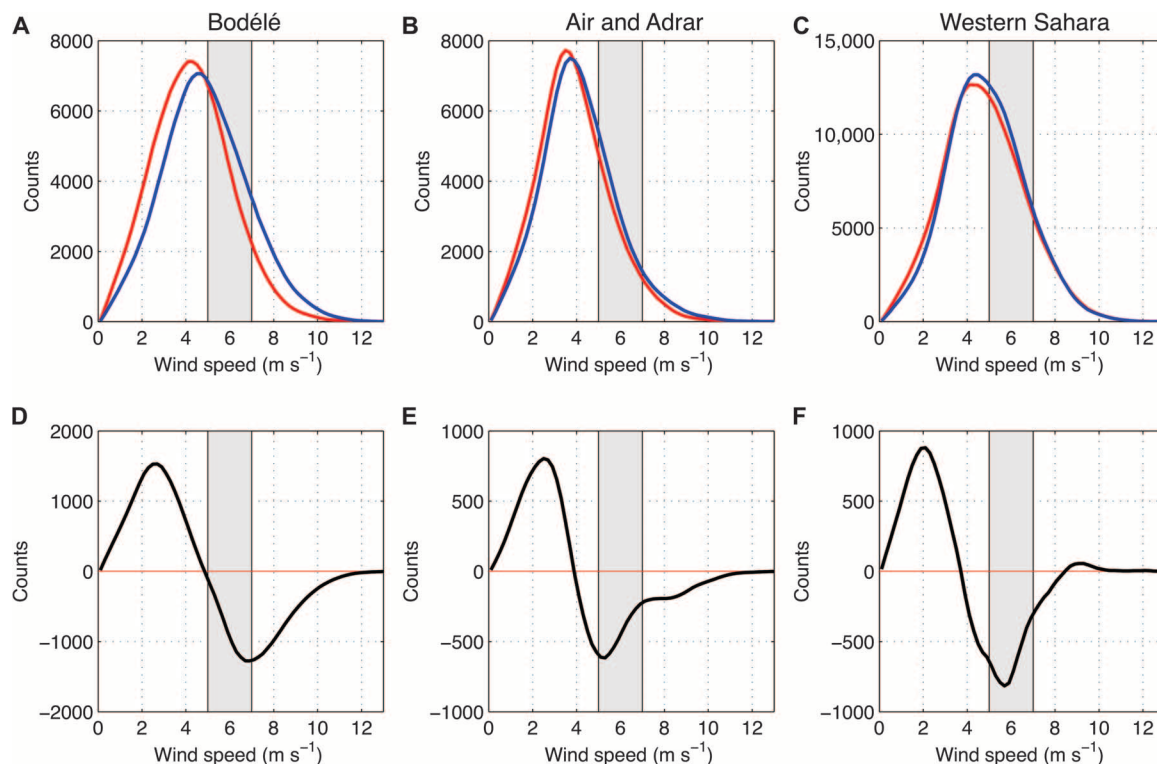


Fig. 3. Wind speed histograms. (A to C) Histogram counts (per 0.2 m s^{-1}) of 10-m wind speed from ERA-Interim reanalysis for the 300 strongest (red) and weakest (blue) phases of the SHL in the Bodélé Depression (A), a depression in the lee of the Air and Adrar Mountains (B), and the Mauritania and Western Sahara (C) in the summertime from 1979 through 2012. The mean values of the wind speed for the strong and weak SHL are statistically significantly different in (A), (B), and (C) based on the t score from a two-tailed t test. (D to F) Wind speed histogram differences for the warm minus cool SHL cases. The gray-shaded region represents wind speed threshold for dust emission. A qualitatively identical shift in the wind speed distribution is also observed during the month of May (not shown).

threshold for dust emission to occur in the Sahara is about 5 to 7 m s^{-1} (15, 26, 27), and thus only changes in the wind speed distribution within and above this threshold range have an effect on dust emission. The climatological 10-m wind speed histograms for the Bodélé (Fig. 3A), Air and Adrar Mountains lee region (Fig. 3B), and Mauritania and Western Sahara (Fig. 3C) source regions all peak at speeds below the threshold for emission. Hence, besides changes in the mean wind speed, changes in tails of the distribution are important for understanding the winds' influence on dust emission.

In all three cases, the difference between the two wind speed histograms (large minus small Z_{hl}) demonstrates that there is a shift in the wind speed distributions over the source regions toward lower wind speeds for larger Z_{hl} (Fig. 3, D to F). Quantitatively, there is a 22.5% (Bodélé), 6.5% (Air and Adrar), and 4.1% (Mauritania and Western Sahara) increase in the frequency of occurrence of wind speeds below the 5 m s^{-1} threshold when comparing large and small Z_{hl} . We find a qualitatively identical shift in the wind speed distribution during the month of May. This reduction in dust emission with an anomalously warm SHL and strong SHL circulation is reflected in the time series of τ_{d} and Z_{hl} (Fig. 1), which are statistically significantly correlated ($r = -0.73$, $P < 0.01$).

DISCUSSION

Our results suggest that the long-noted negative correlation between dust and rainfall is by association and that both features are simultaneously responding to large-scale forcing by the SHL. Such an interpretation of the data is consistent with previous work regarding the influence of the SHL on the physical characteristics of the West African monsoon (21, 23, 24), and with the Ridley *et al.* model (18) and observational studies (10, 16, 25) of North African dust sources. We cannot exclude the possibility that dust emission in Sahel is causally correlated to rainfall via changes in vegetation cover and soil moisture [for example, (15)]; rather we suggest that such effects are to first-order negligible when compared to the coincident changes in dust emission over the vastly larger Sahara.

Finally, when forced with observed sea surface temperatures, climate models are unable to reproduce the observed year-to-year variability of dust over the North Atlantic (8). In light of this work, it is plausible that an underlying cause of this deficiency is an inaccurate representation of the location of the major dust-emitting regions (8). Additionally, initial work (4) suggests that climate models may not sufficiently represent the SHL and its influence on the regional climate, which we have shown is requisite to represent the dust cycle in this part of the world, although more work is needed to comprehensively evaluate the representation of the SHL in climate models.

MATERIALS AND METHODS

Data

Monthly mean τ_{d} , retrieved from satellite radiance measurements from the Advanced Very High Resolution Radiometer, is used to construct the time series of τ_{d} over the northern tropical Atlantic for the summer months (June to August) from 1982 through 2009 (12). In Fig. 1, τ_{d} is averaged over 10° to 65°W and 0° to 30°N . We use monthly mean precipitation data from the Global Precipitation Climatology Project Version 2 to construct the time series of the

Sahel precipitation (21). The precipitation series is averaged over 5°W to 20°E , 10° to 20°N in the summer months (June to August) from 1979 through 2012. We use geopotential height at 925 and 700 hPa at 0600 UT from ERA-Interim daily product to calculate the Z_{hl} , which is the difference in the geopotential heights at these two pressure levels over North Africa (22). Dust emission rates (16) were derived from Spinning Enhanced Visible and Infrared Imager infrared dust index images from March 2006 to February 2008. Last, 925 hPa and 10-m meridional and zonal winds at 0600 UT are from the ERA-Interim daily product from 1979 through 2012. Although wind speeds in the data-sparse Sahara are subject to error, a recent comparison of reanalysis and observed surface winds within the Sahel demonstrated that the ERA-Interim is best suited for analysis of dust emission processes there (28).

Statistical analysis

Correlation coefficients and significance of correlations (using a two-tailed t test) for the time series in Fig. 1 were calculated using the seasonal (June to August) means of each variable and over the time period 1982–2009. We used a Fisher's z transformation to test the statistical significance of the difference between the correlation coefficients of previous- and concurrent-year Sahelian rainfall and τ_{d} . More specifically, this test provides a method of obtaining uncertainty estimates on correlation coefficients, based only on the degrees of freedom in the data. For the zero-lagged correlation between Sahel rainfall and dust, using the 43-year-long Barbados dust data, the correlation coefficient and its 95% confidence interval is 0.53 ± 0.22 , and the same quantity for the 1-year lagged correlation is 0.66 ± 0.18 .

In Fig. 2B, the anomalous wind field was obtained by separate regressions of the meridional and zonal 925-mbar 0600 UT winds onto daily Z_{hl} , using data from the months June to August and the period 1979–2012. Notably, the results in Figs. 2B and 3 (D to F), which were based on daily data, were obtained without first removing the annual cycle in the various data sets examined. However, we were able to reproduce all results after first removing the annual cycles in these data (not shown).

REFERENCES AND NOTES

1. Y. J. Kaufman, I. Koren, L. A. Remer, D. Tanré, P. Ginoux, S. Fan, Dust transport and deposition observed from the Terra-Moderate Resolution Imaging Spectroradiometer (MODIS) spacecraft over the Atlantic Ocean. *J. Geophys. Res.* **110**, D10S12 (2005).
2. A. T. Evan, D. J. Vimont, A. K. Heidinger, J. P. Kossin, R. Bennartz, The role of aerosols in the evolution of tropical North Atlantic Ocean temperature anomalies. *Science* **324**, 778–781 (2009).
3. P. J. DeMott, K. Sassen, M. R. Poellot, D. Baumgardner, D. C. Rogers, S. D. Brooks, A. J. Prenni, S. M. Kreidenweis, African dust aerosols as atmospheric ice nuclei. *Geophys. Res. Lett.* **30**, 1732 (2003).
4. M. Yoshioka, N. M. Mahowald, A. J. Conley, W. D. Collins, D. W. Fillmore, C. S. Zender, D. B. Coleman, Impact of desert dust radiative forcing on Sahel precipitation: Relative importance of dust compared to sea surface temperature variations, vegetation changes, and greenhouse gas warming. *J. Climate* **20**, 1445–1467 (2007).
5. J. M. Creamean, K. J. Suski, D. Rosenfeld, A. Cazorla, P. J. DeMott, R. C. Sullivan, A. B. White, F. M. Ralph, P. Minnis, J. M. Comstock, J. M. Tomlinson, K. A. Prather, Dust and biological aerosols from the Sahara and Asia influence precipitation in the Western U.S. *Science* **339**, 1572–1578 (2013).
6. G. S. Okin, A. R. Baker, I. Tegen, N. M. Mahowald, F. J. Dentener, R. A. Duce, J. N. Galloway, K. Hunter, M. Kanakidou, N. Kubilay, J. M. Prospero, M. Sarin, V. Surapipith, M. Uematsu, T. Zhu, Impacts of atmospheric nutrient deposition on marine productivity: Roles of nitrogen, phosphorus, and iron. *Global Biogeochem. Cycles* **25**, GB2022 (2011).
7. R. Das, A. T. Evan, D. Lawrence, Contributions of long-distance dust transport to atmospheric P inputs in the Yucatan Peninsula. *Global Biogeochem. Cycles* **27**, 167–175 (2013).

8. A. T. Evan, C. Flamant, S. Fiedler, O. Doherty, An analysis of aeolian dust in climate models. *Geophys. Res. Lett.* **41**, 5996–6001 (2014).
9. S. Engelstaedter, I. Tegen, R. Wahsington, North African dust emissions and transport. *Earth-Sci. Rev.* **79**, 73–100 (2006).
10. P. Ginoux, J. M. Prospero, T. E. Gill, N. C. Hsu, M. Zhao, Global-scale attribution of anthropogenic and natural dust sources and their emission rates based on MODIS Deep Blue aerosol products. *Rev. Geophys.* **50**, RG3005 (2012).
11. J. M. Prospero, P. J. Lamb, African droughts and dust transport to the Caribbean: Climate change implications. *Science* **302**, 1024–1027 (2003).
12. A. T. Evan, S. Mukhopadhyay, African dust over the northern tropical Atlantic: 1955–2008. *J. Appl. Meteor. Climatol.* **49**, 2213–2229 (2010).
13. G. R. Foltz, M. J. McPhaden, Impact of Saharan dust on tropical North Atlantic SST. *J. Clim.* **21**, 5048–5060 (2008).
14. F. Fécan, B. Marticorena, G. Bergametti, Parameterization of the increase of the aeolian erosion threshold wind friction velocity due to soil moisture for arid and semi-arid areas. *Ann. Geophys.* **17**, 149–157 (1999).
15. S. M. Cowie, P. Knippertz, J. H. Marsham, Are vegetation-related roughness changes the cause of the recent decrease in dust emission from the Sahel? *Geophys. Res. Lett.* **40**, 1868–1872 (2013).
16. K. Schepanski, I. Tegen, M. C. Todd, B. Heinold, G. Bönisch, B. Laurent, A. Macke, Meteorological processes forcing Saharan dust emission inferred from MSG-SEVIRI observations of subdaily dust source activation and numerical models. *J. Geophys. Res.* **114**, D10201 (2009).
17. P. Knippertz, M. C. Todd, Mineral dust aerosols over the Sahara: Meteorological controls on emission and transport and implications for modeling. *Rev. Geophys.* **50**, RG1007 (2012).
18. D. A. Ridley, C. L. Heald, J. M. Prospero, What controls the recent changes in African mineral dust aerosol across the Atlantic? *Atmos. Chem. Phys.* **14**, 5735–5747 (2014).
19. S. Engelstaedter, R. Washington, Temporal controls on global dust emissions: The role of surface gustiness. *Geophys. Res. Lett.* **34**, L15805 (2007).
20. R. F. Adler, G. J. Huffman, A. Chang, R. Ferraro, P.-P. Xie, J. Janowiak, B. Rudolf, U. Schneider, S. Curtis, D. Bolvin, A. Gruber, J. Susskind, P. Arkin, E. Nelkin, The version-2 global precipitation climatology project (GPCP) monthly precipitation analysis (1979–present). *J. Hydrometeorol.* **4**, 1147–1167 (2003).
21. C. Lavaysse, C. Flamant, S. Janicot, D. J. Parker, J.-P. Lafore, B. Sultan, J. Pelon, Seasonal evolution of the West African heat low: A climatological perspective. *Clim. Dyn.* **33**, 313–330 (2009).
22. D. P. Dee, S. M. Uppala, A. J. Simmons, P. Berrisford, P. Poli, S. Kobayashi, U. Andrae, M. A. Balmaseda, G. Balsamo, P. Bauer, P. Bechtold, A. C. M. Beljaars, L. van de Berg, J. Bidlot, N. Bormann, C. Delsol, R. Dragani, M. Fuentes, A. J. Geer, L. Haimberger, S. B. Healy, H. Hersbach, E. V. Hólm, L. Isaksen, P. Kållberg, M. Köhler, M. Matricardi, A. P. McNally, B. M. Monge-Sanz, J.-J. Morcrette, B.-K. Park, C. Peubey, P. de Rosnay, C. Tavolato, J.-N. Thépaut, F. Vitart, The ERA-Interim reanalysis: Configuration and performance of the data assimilation system. *Q. J. R. Meteorol. Soc.* **137**, 553–597 (2011).
23. C. Lavaysse, C. Flamant, S. Janicot, Regional-scale convection patterns during strong and weak phases of the Saharan heat low. *Atmos. Sci. Lett.* **11**, 255–264 (2010).
24. A. T. Evan, C. Flamant, C. Lavaysse, C. Kocha, A. Saci, Water vapor–forced greenhouse warming over the Sahara desert and the recent recovery from the Sahelian drought. *J. Clim.* **28**, 108–123 (2015).
25. A. T. Evan, S. Fiedler, C. Zhao, L. Menut, K. Schepanski, C. Flamant, O. Doherty, Derivation of an observation-based map of North African dust emission. *Aeolian Res.* **16**, 153–162 (2015).
26. D. L. Westphal, O. B. Toon, T. N. Carlson, A two-dimensional numerical investigation of the dynamics and microphysics of Saharan dust storms. *J. Geophys. Res.* **92**, 3027–3049 (1987).
27. I. Tegen, I. Fung, Modeling of mineral dust in the atmosphere: Sources, transport, and optical thickness. *J. Geophys. Res.* **99**, 22897–22914 (1994).
28. Y. Llargeron, F. Guichard, D. Bouniol, F. Couvreux, L. Kergoat, B. Marticorena, Can we use surface wind fields from meteorological reanalyses for Sahelian dust emission simulations? *Geophys. Res. Lett.* **42**, 2490–2499 (2015).

Acknowledgments: We would like to thank two anonymous reviewers for their helpful comments on an earlier version of this manuscript. **Funding:** This work benefitted from the support of the Agence Nationale de la Recherche (ANR) grant ANR-10-LABX-18-01 of the national Programme Investissements d’Avenir. Funding for this work was also provided by Laboratoire d’excellence Institut Pierre Simon Laplace (L-IPSL). **Author contributions:** W.W. and A.T.E. designed the study. W.W. carried out the main analysis and wrote the manuscript. C.L. provided historical heat low data. All authors discussed the main findings and contributed to the manuscript writeup. **Competing interests:** The authors declare that they have no competing interests. **Data and materials availability:** Reanalysis data from the European Centre for Medium Range Weather Forecasts was downloaded from <http://apps.ecmwf.int/datasets/>. Global Precipitation Climatology Project data were downloaded from the National Climatic Data Center Web site (<http://ncdc.noaa.gov>).

Submitted 20 May 2015

Accepted 31 July 2015

Published 9 October 2015

10.1126/sciadv.1500646

Citation: W. Wang, A. T. Evan, C. Flamant, C. Lavaysse, On the decadal scale correlation between African dust and Sahel rainfall: The role of Saharan heat low–forced winds. *Sci. Adv.* **1**, e1500646 (2015).

This article is published under a Creative Commons license. The specific license under which this article is published is noted on the first page.

For articles published under [CC BY](#) licenses, you may freely distribute, adapt, or reuse the article, including for commercial purposes, provided you give proper attribution.

For articles published under [CC BY-NC](#) licenses, you may distribute, adapt, or reuse the article for non-commercial purposes. Commercial use requires prior permission from the American Association for the Advancement of Science (AAAS). You may request permission by clicking [here](#).

The following resources related to this article are available online at <http://advances.sciencemag.org>. (This information is current as of October 11, 2015):

Updated information and services, including high-resolution figures, can be found in the online version of this article at:

<http://advances.sciencemag.org/content/1/9/e1500646.full.html>

This article **cites 28 articles**, 3 of which you can be accessed free:

<http://advances.sciencemag.org/content/1/9/e1500646#BIBL>

Science Advances (ISSN 2375-2548) publishes new articles weekly. The journal is published by the American Association for the Advancement of Science (AAAS), 1200 New York Avenue NW, Washington, DC 20005. Copyright is held by the Authors unless stated otherwise. AAAS is the exclusive licensee. The title *Science Advances* is a registered trademark of AAAS